EDITORIAL CSIC

Boletín Geológico y Minero
137 (1) january-april 2026, 003
ISSN-L: 0366-0176, eISSN: 2253-6167
https://doi.org/10.21701/bolgeomin/137.1/003

Artículo

Petrographic, petrophysical and engineering geological properties of stone materials employed in the Late Baroque of Val di Noto UNESCO Heritage sites (Sicily, Italy)

Propiedades petrográficas, petrofísicas y geológico-ingenieriles de los materiales pétreos utilizados en los sitios Patrimonio de la Humanidad de la UNESCO del Tardo Barroco de Val di Noto (Sicilia, Italia)

Rosalda Punturo
Department of Biological, Geological and Environmental Sciences, University of Catania, 95129 Catania, Italy. Institute of Environmental Geology and Geoengineering of the National Research Council, Rome, Italy.
rosalda.punturo@unict.it, https://orcid.org/0000-0001-5502-9175

Valeria Indelicato
Department of Biological, Geological and Environmental Sciences, University of Catania, 95129 Catania, Italy. Department of Science, Technology and Society, University School for Advanced Studies Pavia, Piazza della Vittoria, 15 27100, Italy.
https://orcid.org/0000-0001-9440-4038

Simone Mineo
Department of Biological, Geological and Environmental Sciences, University of Catania, 95129 Catania, Italy.
https://orcid.org/0000-0002-7055-4434

Giovanna Pappalardo
Department of Biological, Geological and Environmental Sciences, University of Catania, 95129 Catania, Italy.
https://orcid.org/0000-0002-4979-0459

Gabriele Lanzafame
Department of Biological, Geological and Environmental Sciences, University of Catania, 95129 Catania, Italy.
https://orcid.org/0000-0001-5352-9918

Roberto Visalli
Department of Biological, Geological and Environmental Sciences, University of Catania, 95129 Catania, Italy.
https://orcid.org/0000-0002-6102-4204

Rosolino Cirrincione
Department of Biological, Geological and Environmental Sciences, University of Catania, 95129 Catania, Italy.
https://orcid.org/0000-0002-4595-150X

Abstract: The "late Baroque towns of the Val di Noto" in south-eastern Sicily, Italy, testify an outstanding post-seismic rebuilding architectonic achievement, after that an earthquake destroyed them in 1693. The reconstructed towns, characterised by "distinctive innovations in town planning and urban building" have been added to the UNESCO World Heritage list since 2022. They exhibit architectural features characterised by a close relationship between local stone, geological context and societal development. Indeed, they are characterized by the employment of two lithotypes, i.e., sedimentary (i.e. Hyblean limestones) and magmatic (i.e. Etnean lavas) rocks, resulting in an original bichromy. Nevertheless, once in the city centres, stone materials are exposed to atmospheric agents (e.g., rain, wind, solar radiation, aggressive atmospheric pollutants, freeze-thaw cycles, crystallization of saline solutions, and growth of organisms) that, over time, may trigger weathering process. In this contribution, we focused on two main lithotypes widely used as building stones and, specifically, we carried out a review on its fabric-related petrophysical properties, in terms of petrography, porosity, seismic and geo-engineering behaviour and observed the deterioration forms developed in the buildings. Our review paper aims to provide a basic tool, useful either for conserving monuments of cultural heritage and for their restoration.

Keywords: Limestone; Lavas; UNESCO World Heritage Late Baroque towns; south-eastern Sicily; Italy

Key points:

Late Baroque towns of the Val di Noto" in Italy testify an outstanding architectonic achievement in a unique geological context.

The two main lithotypes are sedimentary (i.e. Hyblean limestones) and magmatic (i.e. Etnean lavas) rocks, resulting in an original two-tone effect.

These rocks are different in terms of petrographic, petrophysical, and geo-engineering behaviour.

Resumen: Los "pueblos del tardo barroco del Val di Noto" en el sureste de Sicilia, Italia, muestran un logro arquitectónico sobresaliente de reconstrucción post-sísmica, después de que un terremoto los destruyera en 1693. Los pueblos reconstruidos, caracterizados por "innovaciones distintivas en planificación urbana y construcción", fueron añadidos a la lista de Patrimonio Mundial de la UNESCO desde 2022. Presentan características arquitectónicas caracterizadas por una estrecha relación entre la piedra local, el contexto geológico y el desarrollo social. De hecho, se caracterizan por el empleo de dos litotipos, rocas sedimentarias (como las calizas "Hyblean") y magmáticas (como las lavas "Etnean"), dando lugar a una bicromía original. Sin embargo, una vez en los centros urbanos, los materiales de piedra están expuestos a agentes atmosféricos (por ejemplo, lluvia, viento, radiación solar, contaminantes atmosféricos agresivos, ciclos de congelación y descongelación, cristalización de soluciones salinas y crecimiento de organismos) que, con el tiempo, pueden desencadenar procesos de meteorización. En este artículo se describen dos litotipos principales ampliamente utilizados como piedra de construcción y, específicamente, se realiza una revisión sobre sus propiedades petrofísicas relacionadas con la estructura, en términos de petrografía, porosidad, comportamiento sísmico y geológico-ingenieril, y se detallan las formas de deterioro desarrolladas en los edificios. El presente artículo de revisión tiene como objetivo proporcionar una herramienta básica, *útil* tanto para conservar monumentos de patrimonio cultural como para su restauración.

Palabras clave: Caliza; Lavas; Ciudades del tardo barroco del Patrimonio Mundial de la UNESCO; sureste de Sicilia; Italia.

Puntos clave:

Los pueblos del tardo barroco del Val di Noto en Italia evidencian un logro arquitectónico sobresaliente en un contexto geológico único.

Los dos litotipos principales son rocas sedimentarias (por ejemplo, calizas Iblicas – "Hyblean") y magmáticas (por ejemplo, lavas etneas "Etnean"), resultando en un efecto de dos tonos original.

Estas rocas son diferentes en términos de comportamiento petrográfico, petrofísico y geológico-ingenieril.

Recibido: 06-05-2024 / **Aceptado**: 06-05-2026 / **Publicado online**: 24-06-2026

Cómo citar: Punturo, R., Indelicato, V., Mineo, S., Pappalardo, G., Lanzafame, G., Visalli, R., Cirrincione, R. (2026). Petrographic, petrophysical and engineering geological properties of stone materials employed in the Late Baroque of Val di Noto UNESCO Heritage sites (Sicily, Italy). Boletín Geológico y Minero, 137(1), 003. http://dx.doi.org/10.21701/bolgeomin/137.1/003

Información complementaria ↓

1. INTRODUCTION

The purpose of the present work is a survey about the typologies of stone materials used in the historical monuments of Eastern Sicily (Italy), their characterization and behavior.

In particular, it is focused on some main lithotypes employed in the "Late Baroque Towns of the Val di Noto" UNESCO World Heritage. Even though most of these cities and towns date back Greek period, their urbanistic setting is modern (18th-19th century) because they were re-built after that an earthquake destroyed them in 1693. Indeed, these towns and cities "*represent a considerable collective undertaking, successfully carried out at a high level of architectural and artistic achievement. Keeping within the late Baroque style of the day, they also depict distinctive innovations in town planning and urban building"* (https://whc.unesco.org/en/list/1024/).

The stone materials employed during the 18^{th}-19^{th} centuries are both magmatic and sedimentary carbonate rocks, which give rise to a characteristic bichromy effect once combined. These rocks were exploited in quarries located in the surrounding areas, showing a close relationship between societal development and geological context (figs.1 A-C).

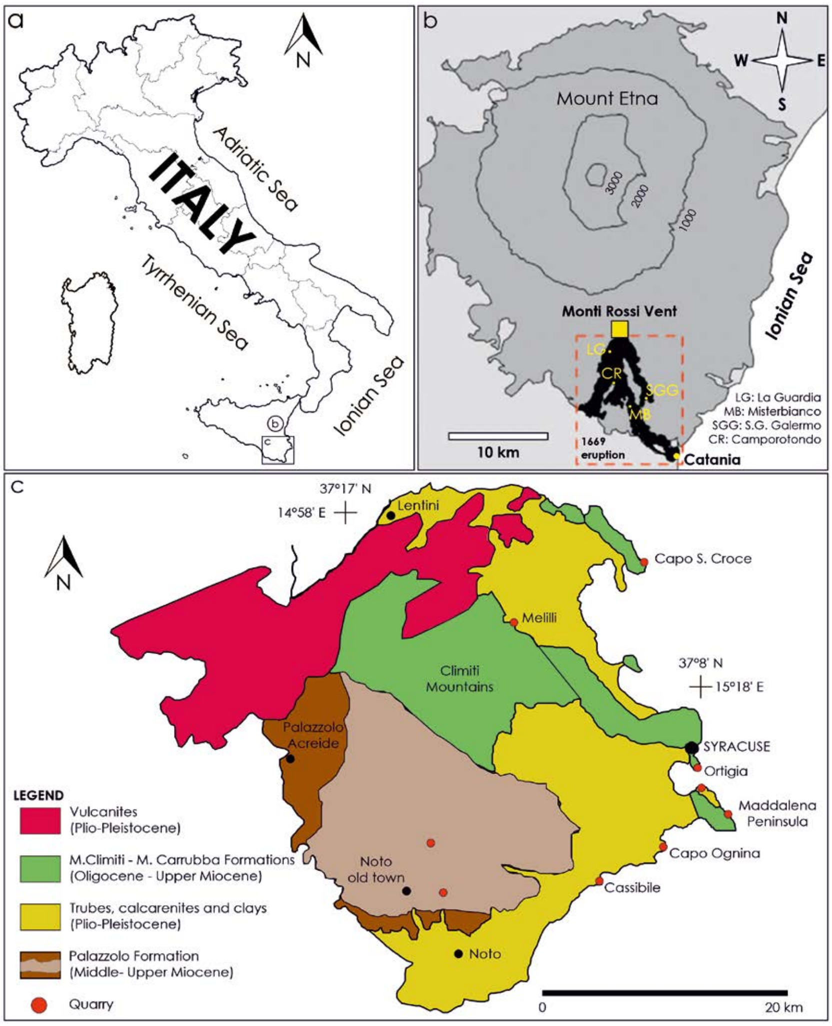

Figure 1. A) Location of the study areas, located in the island of Sicily (Italy). B) schematic map of the Mount Etna volcano (dark grey), location of the Monti Rossi vent (yellow square) and area covered by the 1669 lavas (black) modified from Lanzafame et al. (2022); C) geological sketch map of the Hyblean Plateau (south-eastern Sicily) with red circles indicating the historical quarries of limestone (modified from Punturo et al., 2006).

Figura 1. A) Ubicación de las áreas de estudio, situadas en la isla de Sicilia (Italia). B) mapa esquemático del volcán Monte Etna (gris oscuro), ubicación del conducto Monti Rossi (cuadro amarillo) y área cubierta por las lavas de 1669 (negro), modificado de Lanzafame et al. (2022). C) mapa geológico esquemático de la meseta Íblica (sureste de Sicilia) con círculos rojos que indican las canteras históricas de caliza (modificado de Punturo et al., 2006).

The volcanites are Etnean basalts ("Pietra Nigra"), which are referred to historical 1669 lava flows (Fig.1 B). The 1669 eruption represents by far the largest and most destructive effusive event occurred in historic time at Mount Etna (Branca et al., 2013, 2015). Indeed, the compounded lava field emplaced during 4 months of activity covered a wide area of the southern flank of the volcano, at that time already intensely populated and cultivated. In this paragraph we synthetize the key events of the eruption; a detailed chronology of the 1669 event is reported by Branca et al. (2013) and the impact on the population and the response of the city is discussed in Branca et al. (2015).

Signals of volcanic unrest started on late February 1669, with an increasing seismic activity that caused severe damages to the villages located north of Catania at an elevation between 800 and 600 m a.s.l., forcing the evacuation of the population toward the coast. The eruption started on March 11th in the nearby of the town of Nicolosi with the building of the Monti Rossi scoria cone in the lowest sector of a 1 km long NNW-SSE oriented fracture extending from 950 and 700 m a.s.l.. Lavas rapidly flowed southwards, partially invading the city of Nicolosi and spreading in two major branches once they encountered the ancient volcanic cone of Monpilieri, about 1 km south from the vents. After 72 hours, the western branch divided in two, making a total of 3 main fronts all advancing toward the villages neighbouring Catania. On 25th March, the eastern and western branches stopped their run after having invaded and partially or totally destroyed the villages of La Guardia, Malpasso, Camporotondo and San Giovanni Galermo. The central branch, amply fed by the lavas emitted at Monti Rossi, kept advancing toward the coast, reaching the city of Misterbianco at an altitude of about 300 m a.s.l. at the end of March and directly threatening the city of Catania. The first contact with the 16th century walls of the city occurred in the early-mid April, after 1 month of eruption and about 15 km away from the vent, in the area between the Tindaro and Infetti bastions. Lavas banked the city walls, occasionally breaking into the city with short-living flows, and surrounded the medieval Ursino Castle located outside the walls on a hill facing the Ionian Sea. On April 26th lava flows entered the water, creating a delta that shifted the coastline of about 1 km. The eruption ended on July 11th, after the emission of about 600 x 10^6 m^3 of lavas, the burial of numerous towns and cultivated areas and the formation of a lava field with the exceptional length of 17 km.

Due to the proximity of these lavas to the city center, the historical quarry sites of Etnean lavas are well known (cfr. Patanè & Cristofolini, 1998; Corsaro et al., 1996; Sansone, 1989), and some of them are still active (figs. 2 A-E). The same holds for the Hyblean limestones, whose historical quarries (figs. 2 A-E) sit in the administrative province of Syracuse (south-eastern Sicily). As it may be observed in Figure 1 C, where a geological sketch is presented, the lithostratigraphic succession of the Hyblean area is given by a thick Meso-Caenozoic carbonatic sequence and by Neogenic-Quaternary clastic (carbonate) levels which are interbedded by basic vulcanites, whose age ranges from Trias to Plio-Pleistocene (Carbone et al., 1982; Grasso & Lentini, 1982; Beccaluva et al., 1998; Romagnoli et al., 2015; Maniscalco et al., 2022).

Figure 2. View of historical quarries from which stone materials employed in Late Baroque towns were exploited. Pietra di Noto stone: A) quarry of yellowish limestone and B) bricks cut from large blocks (modified after Pappalardo et al., 2022). C) Quarry of pale-cream limestone. D) Panoramic view and e) detail of one historical quarry sitting on 1669 lavas (modified after Pappalardo et al., 2022).

Figura 2. Vista de canteras históricas de las que se explotaban los materiales de piedra empleados en los pueblos del tardo barroco. Piedra de Noto: A) cantera de caliza amarillenta y B) ladrillos cortados de grandes bloques. C) Cantera de caliza de color crema pálido. D) Vista panorámica. E) Detalle de una cantera histórica situada sobre las lavas de 1669.

The Hyblean limestones are marketed with the general name of "Pietra di Siracusa" and their use in the monuments and religious as well as civil buildings, is related to their different characteristics (e.g., Punturo et al., 2006; Cultrone et al., 2008; Belfiore et al., 2021; Punturo et al., 2023; Occhipinti et al., 2024). Among these limestone lithotypes, it is worth noting that the so-called "Pietra di Noto", exploited in the surroundings of the city of Noto (Fig. 1 C), is widely used (Punturo et al., 2006; Cirrincione et al., 2000; Pappalardo et al., 2016). These limestones are ascribed to the Palazzolo Formation (Carbone et al., 1982; Grasso & Lentini, 1982) and, because of their easy availability and workability have been employed in the monuments either for architectural (figs. 3 A, B) and for decorative elements (figs. 3 C, D); especially in the city of Catania, "Pietra di Siracusa" lythotypes are often combined with the Etnean lavas in a harmonious two-tone effect (figs. 4 A-F), admirable in many religious and civil historical buildings.

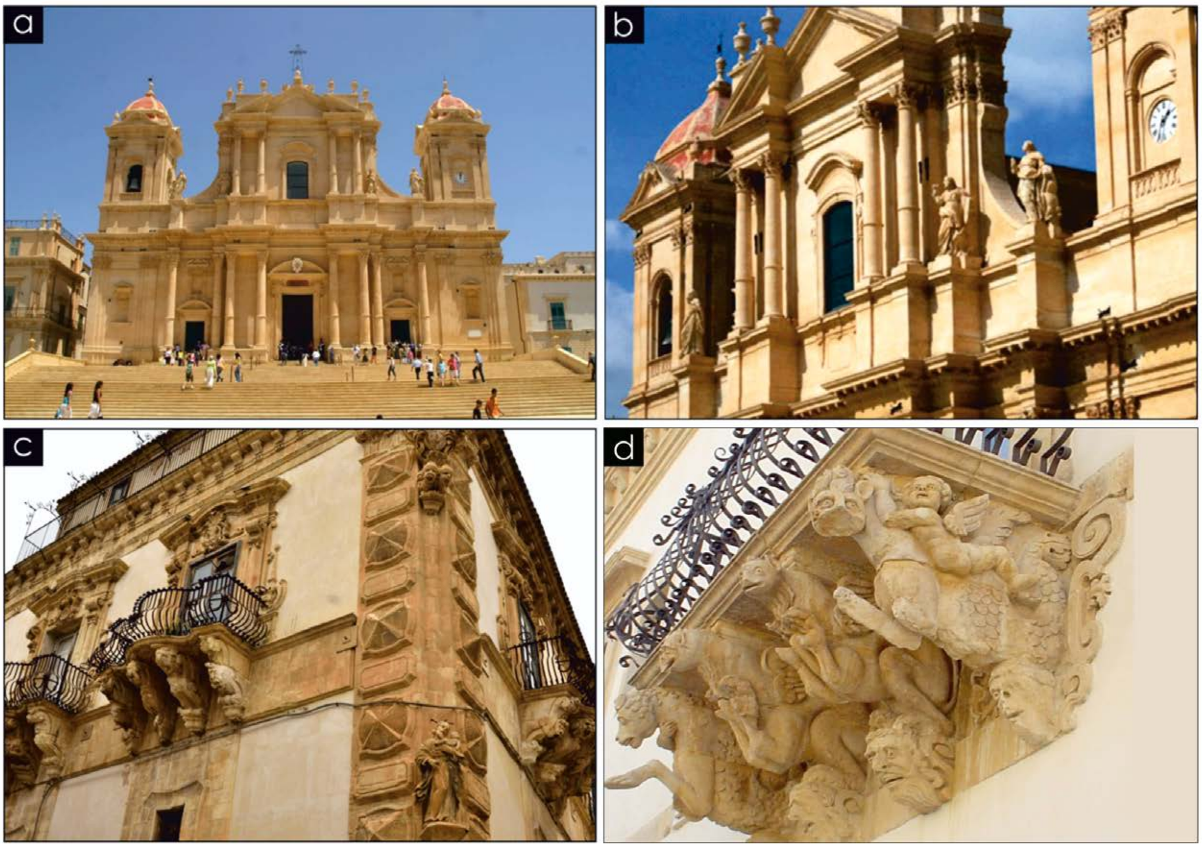

Figure 3. Picture of some representative monuments and edifices of the Late Baroque towns of the Val di Noto UNESCO site. A) Panoramic view of the façade and B) detail of the Cathedral of the city of Noto (photos from https://www.lct-architettura.it/portfolio/ricostruzione-della-cattedrale-di-noto/). C) balcony and pilaster strips of the Palazzo Beneventano (town of Scicli). D) detail of balcony of the Palazzo Beneventano (town of Scicli).

Figura 3. Imagen de algunos monumentos y edificios representativos de los pueblos del tardo barroco del sitio de la UNESCO en el Val di Noto. A) Vista panorámica y B) detalle de la Catedral de la ciudad de Noto (fotos de https://www.lct-architettura.it/portfolio/ricostruzione-della-cattedrale-di-noto/). C) balcón y lesenas del Palazzo Beneventano (ciudad de Scicli).. D) detalle del balcón del Palazzo Beneventano (ciudad de Scicli).

Figure 4. Representative monuments of the city of Catania, showing the typical two-tone effect given by the combined use of limestone and volcanic rocks: A) detail of Ferdinandea gate (also known as “Fortino”, i.e., small fortress). B) detail of the sculptures of the façade of the Benedictine Monastery. C) façade of the Tezzano Palace, also known as “clock’s Palace”. D) Entrance of the Benedictine Monastery edifice. E) Angle view of the Benedictine Monastery. F) Façade of St Demetrio Palace.

Figura 4. Monumentos representativos de la ciudad de Catania, que muestran el típico efecto bicolor obtenido por el uso combinado de piedra caliza y rocas volcánicas: A) detalle de la puerta Ferdinandea (también llamada “Fortino”, es decir, pequeña fortaleza). B) detalle de las esculturas de la fachada del Monasterio Benedictino. C) fachada del Palacio Tezzano, también conocido como “Palacio del Reloj”. D) entrada del edificio del Monasterio Benedictino: e) vista en ángulo del Monasterio Benedictino. F) fachada del Palacio San Demetrio.

2. PETROGRAPHIC, PETROPHYSICAL AND ENGINEERING GEOLOGICAL PROPERTIES

Owing to the historical and architectonic significance of the 1669 lavas and of the Pietra di Noto stones, their petrology, petrography, petrophysics and geo-mechanical characters were previously investigated in different papers (cfr. Corsaro et al., 1996; Mulas et al., 2016; Kahl et al., 2017; Pappalardo et al., 2016, 2017; Magee et al., 2020; Lanzafame et al., 2022; Punturo et al., 2006) by means of Optical Microscopy, Electron Probe Micro Analysis (EPMA), Scanning Electron Microscope imaging (SEM-EDS), synchrotron radiation X-ray 3D computed microtomography (SR-XμCT), ultrasound testing, physical-mechanical laboratory characterization, innovative non-destructive infrared thermography applications.

2.1. “Pietra di Noto” limestone

Pietra di Noto limestones belong to the Palazzolo Formation dating to middle Miocene (Fig. 1 C). There are actually two types: (a) Pale cream limestone and (b) Yellowish limestones (figs 5 A-C), whose main features are hereby reported.

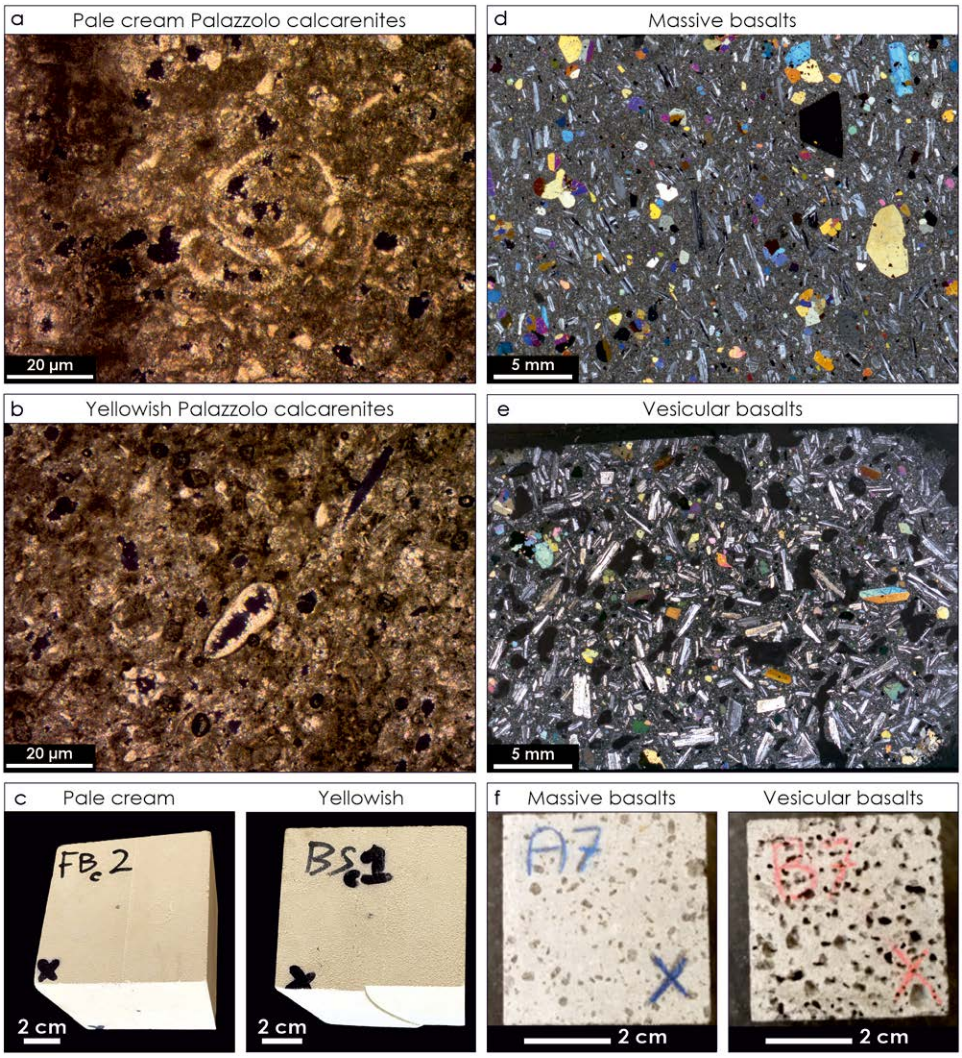

Figure 5. Photomicrographs and sample cubes of the two studied lithotypes employed as building stones. Pietra di Noto limestone: A) pale cream calcarenite, B) yellowish calcarenite and C) sample cubes. Etnean lavas: d) massive basalt, e) vesicular basalt. F) Sample cubes.

Figura 5. Fotomicrografías y cubos de muestra de los dos litotipos estudiados empleados como piedras de construcción. Piedra de Noto. A) Calcarenita de color crema pálido. B) Calcarenita amarillenta y C) cubos de muestra. Lavas Etneas. D) Basalto macizo. E) Basalto vesicular. F) Cubos de muestra.

2.1.1. Petrography and petrology

The classification of the rocks and their porosity description at the scale of the microscope is after Dunham (1962) and Choquette & Pray (1970), respectively.

Pale-cream limestones are bioclastic wackestones with planktonic microfauna (figs. 5 A, C). The grain size is fine calcarenite, with grains floating into the matrix. The bioclasts are mostly planktonic (Globigerinides) and benthonic foraminifers with rare fragments of echinoids, molluscs shells and calcareous algae. The clastic grains are given by quartz and by minor feldspar. The intergranular space is filled by micrite with local crystallization of microsparite. At the scale of the microscope, porosity - both interparticle and vug type and develope within either fossils and matrix (figs. 5 A, F). According to the literature (Carbone et al., 1982; Punturo et al., 2006) this facies belongs to the marine Serravallian-Tortonian carbonate sediment (Palazzolo Formation) the most important historical quarry is the one located nearby Noto town in the S. Corrado di Fuori district (Fig. 1 C).

The Yellowish limestones consist of fine to medium calcarenites. The abundance of the skeletal grains ranges from 10 to 20%; the grains are dominantly planktonic and benthonic foraminifers with rare echinoids, worms calcareous tubes and Bryozoa fragments (figs. 5 B, C). The clastic grains are exclusively represented by quartz. The intergranular space is filled by micrite with local microsparite. The porosity - both interparticle and vug type develops within fossils and matrix. According to the literature (Punturo et al., 2006) this facies was exploited in an old quarry, which is located in the Porcary district nearby Noto.

2.1.2. Petrophysics

The inner 3D structure of the Pietra di Noto representative samples (i.e., BS1, D16, FB2 specimens) was investigated by SR-XμCT at the SYRMEP beamline of the Elettra – Sincrotrone Trieste laboratory in Basovizza (Trieste, Italy) following the same procedure employed in the 1669 lavas described in Lanzafame et al. (2022). In this case, two scans were collected from different zones of each sample. From the tomographic images, the sole pore phase was extracted and analysed (Fig. 6) by pyPore3D software (Aboulhassan et al., 2022). Average results of 2 measurement per sample indicate a pore content of 30.51, 30.66, and 37.04 vol.% for BS1, D16 and FB2, respectively. The seismic behavior of studied rocks under ultrasonic investigation reflects the above reported differences, with P-wave velocity values ranging from a minimum of 2.51 km/s affecting the yellowish limestone specimens (average 2.62 km/s) to a maximum of 3.61 km/s found for pale cream limestones (average 3.40 km/s).

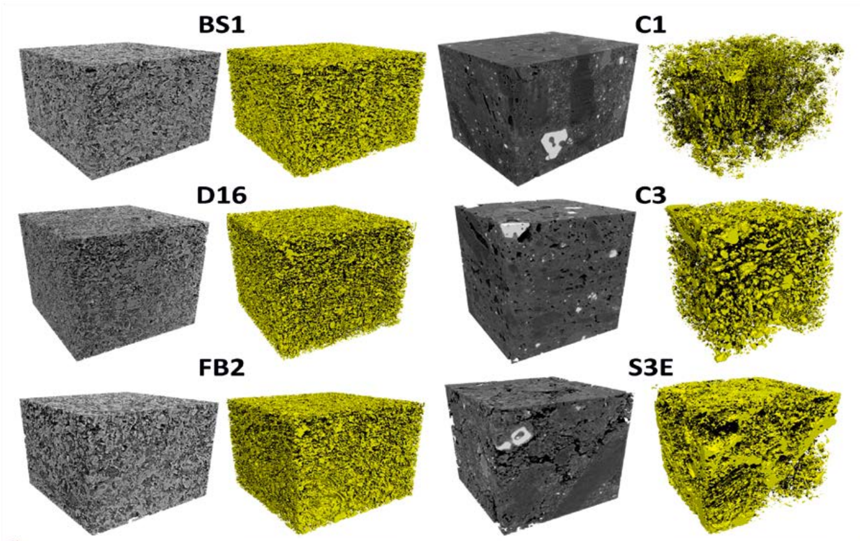

Figure 6. The three-dimensional renderings of the X-ray microtomographic images, showing the investigated volumes of interest (in greyscale) and the extracted pore phase (in yellow). Labels: BS1 and D16 (pale-cream limestone); FB2 (yellowish limestone); C1 (massive lava); C3 and S3E (vesiculated lavas).

Figura 6. Representaciones tridimensionales de las imágenes microtomográficas de rayos X, que muestran los volúmenes de interés investigados (en escala de grises) y la fase porosa extraída (en amarillo). Etiquetas: Bs1 (caliza amarillenta); D16 y FB2 (caliza crema pálido); C1 (lava maciza); C3 y S3E (lavas vesiculadas).

2.1.3. Engineering geological properties

Data commented in this section refer to literature works by Pappalardo et al., (2016, 2022) and Pappalardo & Mineo (2023). Due to the use of such rock type for the reconstruction of Saint Nicholas Cathedral (figs. 3A, B), one of the most acknowledged worship places of Sicily set in the baroque town of Noto, its laboratory characterization was subject of different studies. The two limestone varieties of the Pietra di Noto (i.e., Palazzolo formation), namely the yellowish limestone and the pale-cream limestone are characterized by different engineering geological properties.

Bulk density is, on average, 1775 kg/m^3, with the yellowish Stone affected by the lowest values (1502 kg/m3), index of a less compact rock structure. Average imbibition coefficients are 18% and 12% for yellowish and pale-cream stones, respectively, suggesting a different number of voids in terms of effective and total porosity. Total porosity, estimated through the procedures suggested by EN1936 (1999), is averagely 37% and 29% for yellowish and pale-cream limestones, respectively, while mean effective porosity ranges from 29% and 22%. Therefore, about 80% of the rock porosity is represented by interconnected voids. Porosity was also estimated through the innovative approach of IRTest (after Mineo & Pappalardo, 2016, 2019, 2022), a quick nondestructive procedure based on the thermal infrared rock cooling monitoring (figs. 7 B-D), resulting in average estimated values of 38% and 29.5% for Noto and Palazzolo stones, respectively, in agreement with laboratory measurements.

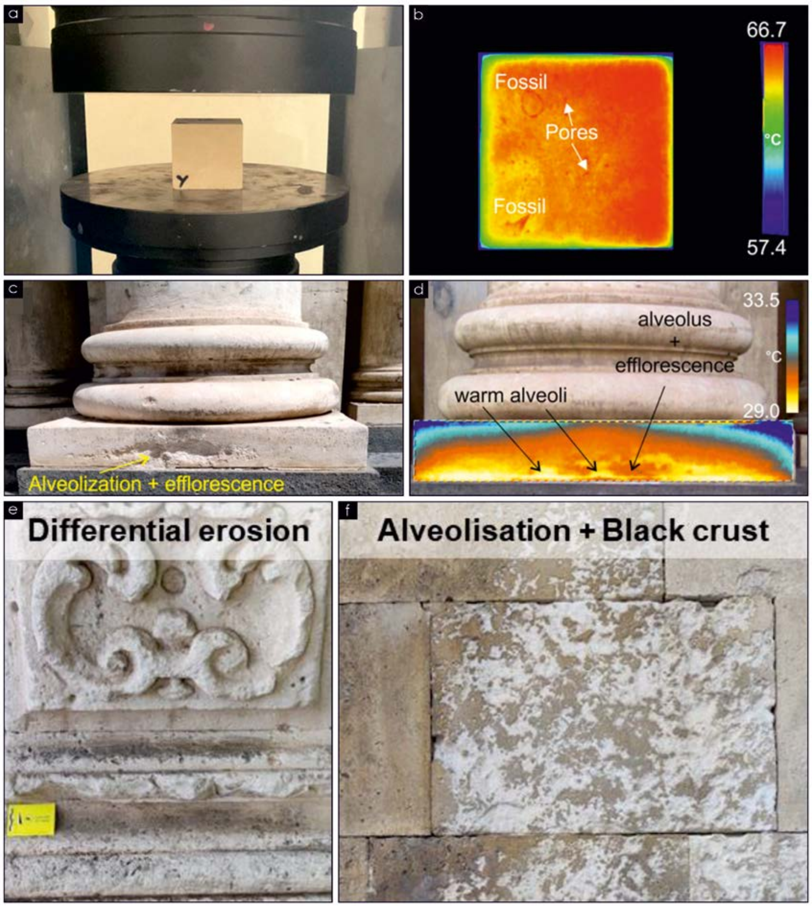

Figure 7. A) Cubical limestone specimen placed in the hydraulic press for mechanical characterization. B) Infrared image of a cubical limestone specimen during the IRTest, with key elements labeled. C) Alveolar weathering and efflorescence surveyed at the stylobate of a column in a historical building of Catania. D) IRT detection of alveoli and efflorescence. E) Detail of differential eroson. F) Detail of alveolisation and black crust development. Images in insets b-c-d are modified after Pappalardo et al. (2022).

Figura 7. A) Espécimen cúbico de piedra caliza colocado en la prensa hidráulica para caracterización mecánica. B) Imagen infrarroja de un espécimen cúbico de piedra caliza durante la prueba IR, con elementos clave etiquetados. C) Meteorización alveolar y eflorescencias observadas en el estilóbato de una columna en un edificio histórico de Catania. D) Detección por IRT de alveolos y eflorescencias. E) Detalle de erosión diferencial. F) Detalle de alveolización y desarrollo de costra negra. Las imágenes en los recuadros b-c-d están modificadas a partir de Pappalardo et al. (2022).

The only common physical property to both varieties is the real density (2650-2700 kg/m3) supporting the rocks provenance from a single geological formation. With reference to the mechanical rock behavior, estimated through Uniaxial Compression Tests (Fig. 7 A), Pale cream limestone proved the strongest and less deformable rock type, with mean UCS of 21 MPa and Young's Modulus (E) of 4.33 GPa, which is about double compared to the yellowish limestone strength (9.7 MPa) and deformability modulus (2.45 GPa).

When these rocks, employed as construction stone, are exposed to meteoric agents, the most common deterioration features are the alveolar (or honeycomb) weathering and the efflorescence (figs. 7 C-F). In the first case, the mechanical limestone disaggregation is enhanced by the rock weak mechanical strength. On the other hand, the rock effective porosity favors the water migration through the pore network, where the precipitation of salt crystals gives rise to the efflorescence and subflorescence. These features were documented in historical buildings even by Infrared Thermography, based on the thermal contrast occurring between warmer cavernous portions (alveoli) and colder salt-crystallized parts (efflorescence, figs. 7 E, F) (Pappalardo et al., 2022).

2.2. Etnean 1669 basalt

2.2.1. Petrography and Petrology

The 1669 lavas display the typical petrologic and petrographic features of the recent trachybasaltic Etnean products.

From the hand scale analysis, rock specimens can be distinguished into massive basalts (figs. 5 D, F), which are characterized by the absence of visible voids, and vesicular basalts (figs. 5 E, F), showing millimetric to centimetric voids arising from degassing processes in the lava flow. They plot in the hawaiite field of the TAS diagram (Le Maitre, 2002) and exhibit porphyritic texture given by phenocrysts of millimetric clinopyroxene (mainly augite and subordinate diopside), plagioclase (with andesinic to bitownitic composition) and sub-millimetric forsterite-rich olivine and Ti-Fe oxides (magnetite), all occurring also as microlites in the groundmass (figs. 5 D, E). Lavas display different number of vesicles that confer a massive (Fig. 5 D) to vesicular aspect (Fig. 5 E) to the rocks (Pappalardo et al., 2017). The porphyritic index (PI = total vol.% of phenocrysts) varies between 29 and 44. The colour index (CI = mafic phenocrysts / total phenocrysts) ranges between 52 and 26 on the basis of the vescicularity, since the most massive variety display a higher abundance of mafic crystals compared to the vesicular ones. Plagioclase is the most abundant mineral phase, with phenocrysts showing both clear and patchy/sieve textured cores (An52-88), direct and oscillatory zoning and clear rims $An_{49\text{-}77}$ (Lanzafame et al., 2022). Clinopyroxenes phenocrysts reach size up to 5 mm (Magee et al., 2020) and show a narrow compositional range ($Wo45_{-47}En_{40-41}Fs_{13-14}$). Some individuals may show twinning and are characterized by either concentric or "hourglass" sector zoning, with fracturing mostly developed along the cleavage system. Olivine is generally weakly zoned, with more forsterite-rich cores (Fo71-77) and Fe-rich rims (Fo46-73). Ti-Fe oxides are mainly titanomagnetite, occurring as phenocrysts and microcrysts in the groundmass or hosted within large clinopyroxenes.

2.2.2. Petrophysics

The porosity of the 1669 lavas has been previously investigated using 2D thin section image analysis (Fig. 4) (Pappalardo et al., 2017) and 3D synchrotron radiation computed microtomography (specimens C1, C3 and S3E; Fig. 5). (Lanzafame et al., 2022) In these papers, authors report a wide range of pores amount spanning from 1 to 32%. Indeed, lavas emitted by the 1669 eruption formed intricate field, characterized by the superimposition of hundreds of single flow units and by an extended network of lava tunnels (Branca et al., 2013; Lanzafame et al., 2022) that imposed different degassing and cooling paths to the flowing melts. The result of this complex genesis is a wide textural variety of the rocks, with massive and almost bubble-free rocks underlying and/or overlying porous ones. The vesicle size and shape remark this heterogeneity, with pores having size going from micrometric or sub-micrometric in the massive rocks to centimetric in the scoriaceous crust of some flows. Voids in lavas are also due to the presence of microcracks that affect both the phenocrysts and groundmass, whose genesis has been related by Pappalardo et al. (2017) to the thermal retraction phenomena affecting large crystals.

Results from compressional wave velocities (Vp) investigation results show that the massive variety is characterized by average Vp ranging from 2.70 to 3.28 km/s, whereas the Vp average values of the vesicular lavas are lower ≈2 km/s.

Results highlight the control of intrinsic (i.e., constituting minerals and their abundances, rock fabric) and extrinsic (i.e., crack and pores) parameters on the elastic behaviour of the rock.

2.2.3. Engineering geological properties

The engineering geological properties of basalts from Mount Etna is commented herein based on literature studies by Pappalardo et al. (2017) and Pappalardo & Mineo (2017). Lava blocks to be employed as construction materials are often quarried along ancient lava flows (figs. 2 D, E). The different vesicular degree observed at the mesoscale (figs. 8 A, B) results in a wide range of bulk density which ranges from 2117 to 2920 kg/m^3. The highest value refers to the massive rocks, while the lowest is typical of basalts affected by centimetric vesicles. Total porosity, estimated through the EN1936 procedure, is very low for massive specimens (on average 5%), while it reaches a 20% mean value at vesicular ones. Even in this case, literature studies report the use of Infrared Thermography to study some rock features in laboratory (figs. 8 C, D), and the porosity estimated through the innovative IRTest returned a comparable average porosity range (Mineo & Pappalardo, 2016). For these kind of rocks, effective porosity is about half of the total porosity.

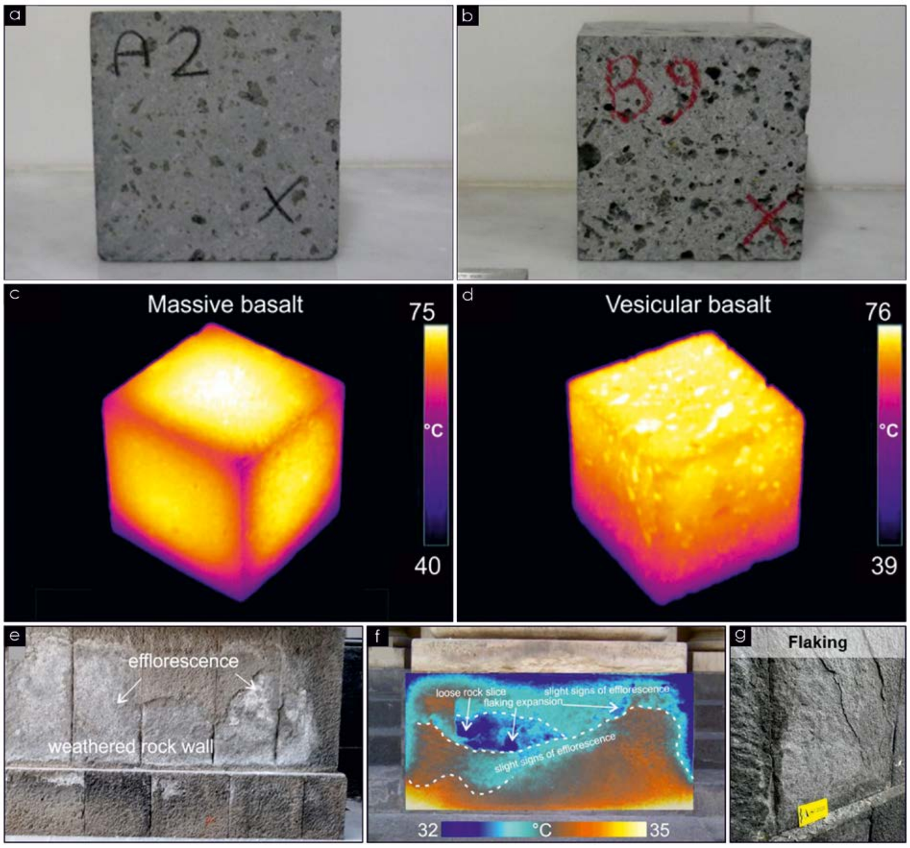

Figure 8. A) Representative massive basalt specimen. B) Representative vesicular basalt specimen. C) IRT view of a massive basalt specimen during IRTesT. D) IRT view of a vesicular basalt specimen during IRTesT. E) Chemical weathering affecting a basaltic building façade. F) IRT detection of efflorescence. G) Detail of flaking. Images in insets e-f are modified after Pappalardo et al. (2022).

Figura 8. A) Muestra representativa de basalto macizo. B) Muestra representativa de basalto vesicular. C) Vista IRT de una muestra de basalto macizo durante IRTesT. D) Vista IRT de una muestra de basalto vesicular durante IRTesT. E) Meteorización química que afecta a la fachada de un edificio de basalto. F) Detección por IRT de eflorescencias. G) Detalle de descamación. Las imágenes en los recuadros e-f están modificadas a partir de Pappalardo et al. (2022).

The analysis of the rock mechanical behavior under uniaxial compression highlighted that UCS and elastic modulus are strongly linked to the rock porosity. As a matter of fact, the strongest rock type is the massive variety, with a 185 MPa mean UCS. On the contrary, the vesicular group offered on average a 71 MPa UCS, due to the presence of voids acting as weakening features. It was also reported that rocks with a low UCS are offer a greater deformation driven by the closure of voids. Average values of elastic modulus range, indeed, from a minimum 6 GPa, found for vesicular rocks, to a maximum 11 GPa of massive specimens.

Despite the good physical mechanical properties of such rock type, weathering may occur as well once employed in outdoor configurations. In particular, saline efflorescence may cause the haloclastic rupture of the rock face, and the overpressure played by crystals can cause the rock exfoliation (Pappalardo et al., 2022). It was observed, indeed, that basalts occurring along the façade of a historical building are affected by mechanical flaking as the consequence of sub-florescence progression (figs. 8 E, G). In the frame of new technological applications to the cultural heritage, the rock flaking can be detected by Infrared Thermography due to the thermal contrast occurring between a sound rock (warm surface temperatures) and detached slice (cold surface temperatures) (Pappalardo et al., 2022; Fig. 8 F).

3. DISCUSSIONS AND CONCLUSION

The characteristic bichromy of the historical monuments of Eastern Sicily (Italy) is due to the employment of the Pietra di Noto limestones displaying light shades and of the black/dark lavas erupted by Mount Etna during the 1669 A.D. eruption.

Among these two types of rocks, some distinctions can be made considering the main textural features. In particular, two types of limestones were employed, one showing pale-cream colour, given by a mix of bioclastic, quartz and feldspar fine grains, and the other displaying yellowish shade and constituted by medium calcarenite grains with bioclastic origin (mostly foraminifera) and quartz grains. The difference in microstructures, nature and amount of the (bio)clasts, together with a variable amount of pores, with the yellowish samples showing a higher presence of voids compared to the pale-cream ones, affect the petrophysical properties, with samples displaying a range of P-wave velocity from ~2.6 km/s for the yellowish limestones to ~3.6 for the pale-cream ones. About the mechanical behavior, the pale cream variety offers the highest UCS, while the yellowish stone, affected by a higher degree of porosity, is the weakest. Also in this case, the dissimilar porosity, which is however represented only by homogeneously distributed pores, seems justifying the diverse mechanical behavior of the two varieties.

Volcanic rocks from Mount Etna from the 1669 A.D. eruption can also be divided in two sub-groups on the basis of the textural features. Indeed, despite their common origin from the same eruptive event, their very similar trachybasaltic composition and mineral assemblage given by plagioclase, pyroxene and olivine, the massive and vesicular types display a different behaviour in petrophysic and mechanical properties because of the different amount of pores, less than 1% in the massive samples and up to 32% in the vesicular ones. This leads to different P-wave velocity, lower (~2 km/s) in the vesicular lavas and higher (up to ~3.3 km/s) in the massive ones. Again, the mechanical behavior of the Etnean rocks is extremely affected by the occurring vesicles; in fact, the highest UCS were found in massive rocks, which also experience a low deformation. It was proven that, for massive specimens, the orientation of microcracks within the rock is responsible of a statistical variability of the engineering geological parameters (Pappalardo et al., 2017). On the other hand, the mechanical behavior of vesicular variety is dependent on vesicles, which also favor the rock deformation.

When both rock types are employed as construction or decorative stones, exposed to meteorological agents, the most common weathering feature is efflorescence, also causing the rock flacking when salt crystallizes within the rock. Besides this, limestones may be affected by alveolar weathering, leading to a differential erosion of the rock face, and by black crust and bioweathering.

Supplementary information ↑

Funding sources

Not applicable.

Supplementary material

Not applicable.

Data availability

Not applicable.

Acknowledgements

Laura Russo and Antonino Lo Giudice are greatly acknowledged for their precious contribution to early studies on Pietra di Noto and Etnean lavas building stone materials. R.P. would like to acknowledge Vincenzo Punturo e Maria Colamino for providing some pictures of the monuments. This research was financially supported by University of Catania, in the frame of "CH2V—Cultural Heritage Hazard and Vulnerability" project, Linea 2-PIACERI, granted to Giovanna Pappalardo. Part of this research benefited of funds by University of Catania (PIAno di inCEntivi per la RIcerca di Ateneo 2020/2022—Pia.Ce.Ri), Grant Number: 22722132153, within the project: "Combined geomatic and petromatic applications: The new frontier of geoscience investigations from field- to micro- scale—(GeoPetroMat)". Physical-mechanical and infrared thermography laboratory tests were carried out at the "Laboratorio di Geologia Applicata"; Petrophysical investigations were carried out at the "Laboratory of Non-Destructive Analysis (L.A.N.D.) both belonging to the University of Catania, Department of Biological, Geological and Environmental Sciences. We acknowledge Elettra Sincrotrone Trieste for providing access to its synchrotron radiation facilities and we thank Giuliana Tromba for assistance in using beamline Syrmep.

Authorship contribution statement

Rosalda Punturo: Conceptualization, Funding acquisition, Investigation, Methodology, Project administration, Writing – review & editing- Photographs / Image editing.

Valeria Indelicato: Formal analysis, Investigation, Writing – original draft_ Photographs / Image editing.

Simone Mineo: Formal analysis, Investigation, Methodology, Writing – original draft- Photographs / Image editing.

Giovanna Pappalardo: Conceptualization, Methodology, Writing – review & editing.

Gabriele Lanzafame: Formal analysis, Investigation, Methodology, Writing – original draft- Photographs / Image editing.

Roberto Visalli: Formal analysis, Investigation, Methodology, Writing – original draft- Photographs / Image editing.

Rosolino Cirrincione: Conceptualization, Writing – review & edit.

Competing interests

The authors of this article declare that they have no financial, professional, or personal conflicts of interest that could have inappropriately influenced this work.

Statement on the use of Artificial Intelligence

Not applicable.

REFERENCES

Aboulhassan, A., Brun, F., Kourousias, G., Lanzafame, G., Voltolini, M., Contillo, A. & Mancini, L. (2022). PyPore3D: an open source software tool for imaging data processing and analysis of porous and multiphase media. Journal of Imaging, 8, 187, doi.org/10.3390/jimaging8070187.

ASTM Standard D2845-00 (2000). Standard Test Method for Laboratory Determination of Pulse Velocities and Ultrasonic Elastic Constants of Rock: D2845-00. Book of ASTM.

Beccaluva, L., Siena, F., Coltorti, M., Grande, A. D., Giudice, A. L., Macciotta, G., Tassinari, R. & Vaccaro, C. (1998). Nephelinitic to tholeiitic magma generation in a transtensional tectonic setting: an integrated model for the Iblean volcanism, Sicily. Journal of Petrology, 39(9), 1547-1576, doi.org/10.1093/petroj/39.9.1547.

Belfiore, C. M., Calabrò, C., Ruffolo, S. A., Ricca, M., Török, Á., Pezzino, A. & La Russa, M. F. (2021). The susceptibility to degradation of stone materials used in the built heritage of the Ortygia island (Syracuse, Italy): A laboratory study. International Journal of Rock Mechanics and Mining Sciences, 146, 104877, doi.org/10.1016/j.ijrmms.2021.104877.

Branca, S., De Beni, E. & Proietti, C. (2013). The large and destructive 1669 AD eruption at Etna volcano: reconstruction of the lava flow field evolution and effusion rate trend. Bulletin of Volcanology, 75, 694-710, doi.org/10.1007/s00445-013-0694-5.

Branca, S., Azzaro, R., De Beni, E., Chester, D. & Duncan, A. (2015). Impacts of the 1669 eruption and the 1693 earthquakes on the Etna region (eastern Sicily, Italy): an example of recovery and response of a small area to extreme events. Journal of Volcanology and Geothermal Research, 303, 25-40, doi.org/10.1016/j.jvolgeores.2015.07.020.

Carbone, S., Grasso, M. & Lentini, F. (1982). Considerazioni sull’evoluzione geodinamica della Sicilia sud-orientale dal Cretaceo al Quaternario. Memoria Società Geologica Italiana, 24, 367-386.

Choquette, P. W. & Pray, L. C. (1970). Geologic nomenclature and classification of porosity in sedimentary carbonates. American Association of Petroleum Geologists, 54(2), 207-250.

Cirrincione, R., Lombardo, T., Mattina, D., Mazzoleni, P. & Pezzino, A. (2000). I materiali lapidei utilizzati nel chiostro di levante del monastero di S Nicolò L’Arena di Catania e considerazioni sul loro degrado. Bollettino delle sedute della Accademia Gioenia di Scienze Naturali in Catania, 33(357), 175-186.

Corsaro, R. A., Cristofolini, R. & Patanè, L. (1996). The 1669 eruption at Mount Etna: chronology, petrology and geochemistry, with inferences on the magma sources and ascent mechanisms. Bulletin of Volcanology, 58, 348-358, doi.org/10.1007/s004450050144.

Cultrone, G., Russo, L. G., Calabrò, C., Uroševič, M. & Pezzino, A. (2008). Influence of pore system characteristics on limestone vulnerability: a laboratory study. Environmental geology, 54, 1271-1281, doi.org/10.1007/s00254-007-0909-1.

Dunham, R. J. (1962). Classification of carbonate rocks according to the depositional texture. In: Ham WE (ed). Classification of carbonate rocks. American Association of Petroleum Geologists Memoir, 1, 108-121.

EN 1936 (1999). Natural Stone Test Methods – Determination of Real Density and Apparent Density, and of Total Open Porosity. European Committee for Standardization, Brussels.

Grasso, M. T. & Lentini, F. (1982). Sedimentary and tectonic evolution of the eastern Hyblean Plateau (southeastern Sicily) during late Cretaceous to Quaternary time. Palaeogeography, Palaeoclimatology, Palaeoecology, 39(3-4), 261-280, doi.org/10.1016/0031-0182(82)90025-6.

Kahl, M., Viccaro, M., Ubide, T., Morgan, D.J. & Dingwell, D. B. (2017). A branched magma feeder system during the 1669 eruption of Mt Etna: evidence from a time-integrated study of zoned olivine Phenocryst populations. Journal of Petrology, 58(3), 443-472, doi.org/10.1093/petrology/egx022.

Lanzafame, G., Giacomoni, P. P., Casetta, F., Mancini, L., Iezzi, G., Coltorti, M. & Ferlito, C. (2022). Degassing, Crystallization and Rheology of Hawaiitic Lava Flows: the Case of the 1669 AD Eruption of Mount Etna (Italy). Journal of Petrology, 63, 1-21, doi.org/10.1093/petrology/egac115.

Le Maitre, R. (2002). Igneous Rocks: a Classification and Glossary of Terms. CUP, doi.org/10.1017/CBO9780511535581.

Magee, R., Ubide, T. & Kahl, M. (2020). The lead-up to Mount Etna's most destructive historic eruption (1669). Cryptic recharge recorded in Clinopyroxene. Journal of Petrology, 61, egaa025, doi.org/10.1093/petrology/egaa025.

Maniscalco, R., Fazio, E., Punturo, R., Cirrincione, R., Di Stefano, A., Distefano, S., Forzese, M., Lanzafame, G., Leonardi, G. S., Montalbano, S., Pellegrino, A. G. & Reale, A. (2022). The porosity in Heterogeneus Carbonate Reservoir Rocks: Tectonic versus Diagenetic Imprint – A Multi-Scale Study from the Hyblean Plateau (SE Sicily, Italy). Geosciences, 12(4), 149, doi.org/10.3390/geosciences12040149.

Mineo, S. & Pappalardo, G. (2016). The Use of Infrared Thermography for Porosity Assessment of Intact Rock. Rock Mechanics and Rock Engineering, 49(8), 3027-3039, doi.org/10.1007/s00603-016-0992-2.

Mineo, S. & Pappalardo, G. (2019). InfraRed Thermography presented as an innovative and non-destructive solution to quantify rock porosity in laboratory. International Journal of Rock Mechanics and Mining Sciences, 115, 99-110, doi.org/10.1016/j.ijrmms.2019.01.012.

Mineo, S. & Pappalardo, G. (2022). Nondestructive rock porosity estimation by InfraRed Thermography applied to natural stones. Construction and Building Materials, 342, 127950, doi.org/10.1016/j.conbuildmat.2022.127950.

Mulas, M., Cioni, R., Andronico, D. & Mundula, F. (2016). The explosive activity of the 1669 Monti Rossi eruption at Mt. Etna (Italy). Journal of Volcanology and Geothermal Research, 328, 115-133, doi.org/10.1016/j.jvolgeores.2016.10.012.

Occhipinti, R., Lazzara, G., Mazzoleni, P., Motta, A. & Barone, G. (2024). Sustainable Protective Strategies and Biocide Applications in the Restoration of Palazzo Centrale Dell'Università, Catania, Italy. Sustainability, 16(7), 2948, doi.org/10.3390/su16072948.

Pappalardo, G., Mineo, S. & Monaco, C. (2016). Geotechnical characterization of limestones employed for the reconstruction of a UNESCO world heritage Baroque monument in southeastern Sicily (Italy). Engineering Geology, 212, 86-97, doi.org/10.1016/j.enggeo.2016.08.004.

Pappalardo, G. & Mineo, S. (2017). Investigation on the mechanical attitude of basaltic rocks from Mount Etna through InfraRed Thermography and laboratory tests. Construction and Building Materials, 134, 228-235, doi.org/10.1016/j.conbuildmat.2016.12.146.

Pappalardo, G., Punturo, R., Mineo, S. & Contrafatto, L. (2017). The role of porosity on the engineering geological properties of 1669 lavas from Mount Etna. Engineering Geology, 221, 16-28, doi.org/10.1016/j.enggeo.2017.02.020.

Pappalardo, G., Mineo, S., Caliò, S. & Bognandi, A. (2022). Evaluation of Natural Stone Weathering in Heritage Building by Infrared Thermography. Heritage, 5(3), 2594-2614, doi.org/10.3390/heritage5030135.

Pappalardo, G. & Mineo, S. (2023). Physical-mechanical characterization of carbonate rocks used for the reconstruction of Saint Nicholas Cathedral in Noto (south-eastern Sicily, Italy). International Scientific Conference Man and Karst 2022 September 12th /- 17th Custonaci, Italy, Speleologia Iblea (Vol. XVII), pp. 109-121.

Patanè, L. & Cristofolini, R. (1998). L'attività estrattiva della zona etnea. Quarry Construction, 8, 5-16.

Punturo, R., Russo, L. G., Giudice, A. L., Mazzoleni, P., Pezzino, A., Trovato, C. & Vinciguerra, S. (2005). I materiali lapidei utilizzati nei monumenti d'epoca tardo barocca del centro storico di Catania: caratterizzazione e stato di degrado. In, MMVI ARACNE (ed). L'approccio multidisciplinare allo studio e alla valorizzazione dei Beni Culturali, Atti del workshop, Siracusa, 28-29 ottobre 2005, pp 347-356. ISBN 88-548-0917-9.

Punturo, R., Russo, L. G., Giudice, A. L., Mazzoleni, P. & Pezzino, A. (2006). Building stone employed in the historical monuments of Eastern Sicily (Italy). An example, the ancient city centre of Catania. Environmental Geology, 50, 156-169, doi.org/10.1007/s00254-006-0195-3.

Punturo, R., Indelicato, V., Lanzafame, G., Maniscalco, R., Fazio, E., Bloise, A., Muschella, L. & Cirrincione, R.

(2023). Petrographic, microstructural and petrophysical study of asphaltic limestone employed in the Late Baroque towns of the Val di Noto UNESCO site (south-eastern Sicily). Construction and Building Materials, 371, 130730, doi.org/10.1016/j.conbuildmat.2023.130730.

Romagnoli, G., Catalano, S., Pavano, F. & Tortorici, G. (2015). Geological map of the Tellaro River Valley (Hyblean Foreland, southeastern Sicily, Italy). Journal of Maps, 11(1), 66-74.

Sansone, I. (1989). Tradizione ed attività del basalto etneo. Tecnica e ricostruzione 4, 3-14.

UNESCO World Heritage list: https://whc.unesco.org/en/list/1024/.

Table 1. Average values of the main geotechnical parameters estimated for each lithotype.

Tabla 1. Valores medios de los principales parámetros geotécnicos de cada litotipo.

	Total porosity (%)	Effective porosity (%)	Bulk density (kg/m3)	Real density (kg/m3)	UCS (MPa)	Young's modulus (GPa)	Vp (km/s)
Yellowish limestones	37	29	1660	2700	9.7	2.45	2.62
Pale cream limestones	29	22	1890	2650	21	4.3	3.40
Basalts massive	5	2	2780	3000	185	11	2.70 to 3.28
Basalts vesicular	20	10	2340	3000	71	6	≈ 2.0